INTEGRATED GEOPHYSICAL INTERPRETATION OF BEDROCK GEOLOGY, SAN ANDRES MOUNTAINS, NEW MEXICO

TIMOTHY J. MACIEJEWSKI

Department of Geological Sciences

APPROVED:

Dr. K. C. Miller, Chair

Dr. G. R. Keller

Dr. G. C. Ohlmacher

Dr. J. Walton

Associate Vice President for Research and Graduate Studies

INTEGRATED GEOPHYSICAL INTERPRETATION OF BEDROCK GEOLOGY, SAN ANDRES MOUNTAINS, NEW MEXICO

by

Timothy J. Maciejewski, B.S.

THESIS

Presented to the Faculty of the Graduate School of

The University of Texas at El Paso

in Partial Fulfillment

of the Requirements

for the Degree of

MASTER OF SCIENCE

Department of Geological Sciences

UNIVERSITY OF TEXAS AT EL PASO

December, 1996

ACKNOWLEDGEMENTS

The list of people who have helped me in one way or another with this thesis is long and distinguished. The primary help came from my committee chairman, Dr. Kate Miller, who thought of me when NASA approached her with the project, and whose knowledge of the ProMax system made the synthetic seismograms possible. Dr. Greg Ohlmacher assisted me with geologic interpretations. Mike Jacobs and Geoff Giles at the NASA–WSTF were very helpful in providing me with all of the data used in this project. Dr. Randy Keller provided me the financial means to get through my undergraduate and graduate degrees. I would also like to thank all of the nameless people who put up with me when I was first learning the UNIX system. Don Roberts and later Carlos Montana kept the UNIX system operating. Alex Duran read, laughed at, and corrected my first attempts at this thesis; and I want to thank Michael and Julie Whitelaw for just being friends.

A special thanks goes to my wife, Diana, for putting up with my coming home late, and working so that I could finish my degree.

This study was partially supported by the NASA–WSTF, New Mexico, and the NASA funded Pan American Center for Earth and Environmental Studies. I would also like to thank the Society of Exploration Geophysicists for giving me a scholarship which helped with tuition payments.

This thesis was submitted to committee on August 21, 1996.

ABSTRACT

During the 1960's and 70's, hazardous materials were released onto the ground surface at the National Aeronautics and Space Administration – White Sands Test Facility (NASA–WSTF) northeast of Las Cruces, New Mexico. Currently, NASA is seeking to identify and classify the nature and extent of the geologic units that influence migration of the hazardous constituents released at this facility. This thesis is part of this effort, and focuses on mapping the top of bedrock and any features contained within the bedrock and overlying alluvium which may influence groundwater flow in the vicinity of the facility.

Approximately 42 miles (67.6 km) of shallow seismic reflection data, well log information from over 80 wells, and a local gravity survey, were used to produce a new top of bedrock map. Several features on this map may affect groundwater flow. Remotely sensed data were used to examine the bedrock lithology and drainage patterns. There are three major faults crossing NNW across the facility, two of which combine to form the eastern boundary fault for the Jornada basin. There are two types of bedrock encountered through drilling on the NASA–WSTF, Tertiary andesite to the west and Paleozoic marine deposits to the east. Gravity modeling shows that the eastern basin boundary fault juxtaposes Paleozoic marine deposits against Tertiary volcanics. This fault has around 7900 ft (2400 m) of displacement. This same model also constrained the Western Boundary Fault Zone–1 to around 1700 ft (517 m) of down to the west displacement, producing a maximum alluvial thickness in the Jornada basin of 2600 ft (790 m).

Several minor faults and natural paleo–topographic features combine to produce two paleochannels trending westward away from the San Andres Mountains. Groundwater may be funnelled into these depressions by natural bedrock topography and faults, and channeled off to the west along with the contaminants.

TABLE OF CONTENTS

ACKNOWLEDGEMENTS iii

ABSTRACT iv

TABLE OF CONTENTS vi

LIST OF FIGURES ix

LIST OF TABLES xii

LIST OF ENCLOSURES xiii

INTRODUCTION 1

REGIONAL GEOLOGY 7

Geologic History 7

Geographical and Structural Settings 13

HYDROLOGY 19

Introduction 19

Hydrologic Overview 19

Contamination Source Areas 24

100 Area 30

200 Area 30

300–400 Areas 30

600 Area 31

700 Area 31

Other Contaminants 31

Modeling Methods 32

BEDROCK INTERPRETATION FROM SEISMIC RECORDS AND WELL DATA 35
Mapping Methods 35
Seismic Introduction 36
Bedrock Composition 38
Major Faults 41
Western Boundary Fault Zone 1 (WBFZ–1) 42
Hardscrabble Hill Fault 42
Western Boundary Fault Zone 2 (WBFZ–2) 44
200–East and 200–West Fault 43
Detailed Structure of the On–site Areas 46
100 Area 46
200 Area 47
300 Area 50
400 Area 50
600 Area 50
700 Area 52
Paleochannels 52
Bedrock Features of the Offsite Region 56
Depth to Bedrock 57
Implications of Bedrock Map for Site Geology and Hydrology 57
SEISMIC SIGNATURE OF THE BEDROCK 63
Log information 63
GRAVITY AND MAGNETICS 80
Introduction 80

Gravity Acquisition and Processing 80
NASA–WSTF Gravity Map 83
Regional Gravity Map 85
Magnetics 85
Gravity Modeling 88
REMOTE SENSING 99
Purpose 99
Introduction 99
Data Involved 100
Thematic Mapper regional 100
Thematic Mapper local 103
Terrain Draped with Gravity 105
CONCLUSIONS 107
REFERENCES 109
APPENDIX A: VERTICAL SEISMIC PROFILE 112
Introduction 112
Data Acquisition 112
Data Interpretation 113
APPENDIX B: WELL LOCATION AND BEDROCK LITHOLOGY 118
CURRICULUM VITAE 123

LIST OF FIGURES

Figure 1. NASA–WSTF location map. 2

Figure 2. Seismic lines, contamination source points, and monitoring wells within the NASA–WSTF. 4

Figure 3. Monitoring well names. 5

Figure 4. Paleotectonics of the southern Cordillera and Ouachita. 8

Figure 5. Stratigraphic column for the San Andres mountains (pC – Perm.). 9

Figure 6. Stratigraphic column for the San Andres mountains (Perm – Quat.). . . 10

Figure 7. Regional structures of the NASA–WSTF. 15

Figure 8. Cross sections of the western San Andres mountains and Jornada basin from Seager, 1981. 16

Figure 9. Bedrock outcrop map in the eastern most portion of the NASA–WSTF. 18

Figure 10. Hydrogeologic cross section of bedrock and alluvium from GCL 1995. 21

Figure 11. Saturated alluvial isopach map. 22

Figure 12. Listing of hydrostratigraphic, lithostratigraphic and hydrostratigraphic units occurring on the facility. 23

Figure 13. Water table map. 25

Figure 14. Water recharge locations and a portion of the 3DSWBM 27

Figure 15. Distribution of Freon–113. 29

Figure 16. Vertical cross section of the 3DSWBM discretization. 33

Figure 17. Elevation map. 39

Figure 18. Bedrock type of the onsite region. 40

Figure 19. Elevation of the bedrock in the 100 and 600 areas. 45

Figure 20. Elevation of the bedrock in the 200, 300, and 400 areas. 48

Figure 21. Stresses induced during the Rio Grande Rift. 49

Figure 22. Elevation of the bedrock in the 300, 400, and 700 areas. 51

Figure 23. Location of paleochannels within the NASA–WSTF. 53

Figure 24. Bedrock paleochannels with Freon–113 contamination plume. 55

Figure 25. Alluvial isopach map. 58

Figure 26. Cross section of the NASA–WSTF. 59

Figure 27. Location of 200–F, 200–G, and 600–D wells. 64

Figure 28. Density and sonic logs data for the 200–F well. 66

Figure 29. Impedance and reflection coefficients for the 200–F well. 67

Figure 30. Density and sonic logs data for the 200–G well. 68

Figure 31. Impedance and reflection coefficients for the 200–G well. 69

Figure 32. Density and sonic logs data for the 600–D well. 70

Figure 33. Impedance and reflection coefficients for the 600–D well. 71

Figure 34. Example of filter panels for the 600–D synthetic. 73

Figure 35. Synthetic seismogram from the 200–F well. 74

Figure 36. Synthetic seismogram from the 200–G well. 75

Figure 37. Synthetic seismogram from the 600–D well. 76

Figure 38. Comparison synthetic seismogram of 200–F to GC–11. 78

Figure 39. Comparison of raw shot record to line GC–2. 79

Figure 40. Location of old and new gravity stations. 81

Figure 41. Local bouguer gravity contour map. 84

Figure 42. Regional bouguer gravity contour map. 86

Figure 43. Contoured magnetic data from the UTEP database. 87

Figure 44. Contoured magnetic data from 1995 survey. 89

Figure 45. Grey scale magnetic map. 90

Figure 46. Gravity model of the Jornada basin. 92

Figure 47. Gravity model of the Jornada basin from Gilmer et al., 1986. 93

Figure 48. Thematic mapper false color regional map, bands 3, 4, and 7. 102

Figure 49. TM false color image of the NASA–WSTF, bands 1, 5, and 7. 104

Figure 50. A 2–Dimensional view of the San Andres Mountain topography draped with Bouguer gravity data. 106

Figure 51. Vertical seismic profile for well 600–D. 114

LIST OF TABLES

Table 1. Contaminant name, chemical name, and maximum concentration recorded in the groundwater. 26

Table 2. Depth to velocity conversion table. 36

Table 3. Well log depth and bedrock type encountered for the three wells of interest. 65

Table 4. Density of bedrock formations used for gravity modelling. 94

Table 5. Spectral bands of the TM images and their respective wavelengths. . . . 100

Table A–1. Time and Velocity information from the vertical seismic profile on the 600–D well. 116

LIST OF ENCLOSURES

Enclosure 1.	Final Bedrock Elevation Contour Map.
Enclosure 2.	Interpreted seismic line GC – 1.
Enclosure 3.	Interpreted seismic line GC – 2.
Enclosure 4.	Interpreted seismic line GC – 3.
Enclosure 5.	Interpreted seismic line GC – 4.
Enclosure 6.	Interpreted seismic line GC – 5, 12.
Enclosure 7.	Interpreted seismic line GC – 6.
Enclosure 8.	Interpreted seismic line GC – 7.
Enclosure 9.	Interpreted seismic line GC – 8.
Enclosure 10.	Interpreted seismic line GC – 9.
Enclosure 11.	Interpreted seismic line GC – 10.
Enclosure 12.	Interpreted seismic line GC – 11.
Enclosure 13.	Interpreted seismic line GC – 13.
Enclosure 14.	Interpreted seismic line GC – 14.
Enclosure 15.	Interpreted seismic line GC – 15.
Enclosure 16.	Interpreted seismic line GC – 16.
Enclosure 17.	Interpreted seismic line GC – 17.
Enclosure 18.	Interpreted seismic line GC – 18.
Enclosure 19.	Interpreted seismic line GC – 19.

Enclosure 20. Interpreted seismic line GC – 20.

Enclosure 21. Interpreted seismic line GC – 21.

Enclosure 22. Interpreted seismic line GC – 22.

Enclosure 23. Interpreted seismic line GC – 23.

Enclosure 24. Interpreted seismic line GC – 24.

Enclosure 25. Interpreted seismic line GC – 25.

Enclosure 26. Interpreted seismic line GC – 26.

INTRODUCTION

Since the establishment of the National Aeronautic Space Administration White Sand Test Facility (NASA–WSTF) in 1964, there have been few studies of the local geology. Questions still remain about the location and displacement of faults within the Jornada basin. It is these faults that control the location and type of bedrock beneath the NASA–WSTF. The top of bedrock controls the flow direction of the groundwater and the type of bedrock could significantly effect the rate of groundwater flow through the bedrock.

Site–specific hydrologic processes are important at the NASA–WSTF as propellants and solvents have been either accidently or purposely disposed of on the surface of the ground and stored in leaking underground storage tanks (LUSTS) over a number of years. Ground surface contamination and dumping has caused a plume of contaminants to enter and be carried along with the groundwater. NASA is now required to characterize the hydrologic cycle through the NASA–WSTF, in order to model the contaminant plumes through time. This model is part of a report from NASA to the Environmental Protection Agency (EPA) as part of a Resource Conservation Recovery Act (RCRA) Facility Investigation/Corrective Measure Study (RFI/CMS). This becomes important when one considers that the third–most populous city in New Mexico, Las Cruces, is less then 18 miles (29.0 km) to the southwest of the NASA–WSTF (Figure 1). This thesis combines additional local data and regional geologic information in order to present a more detailed picture of geology which may affect the hydrologic flow under the site. A subset of these results were used by the NASA–WSTF in their report to the EPA early in 1996.

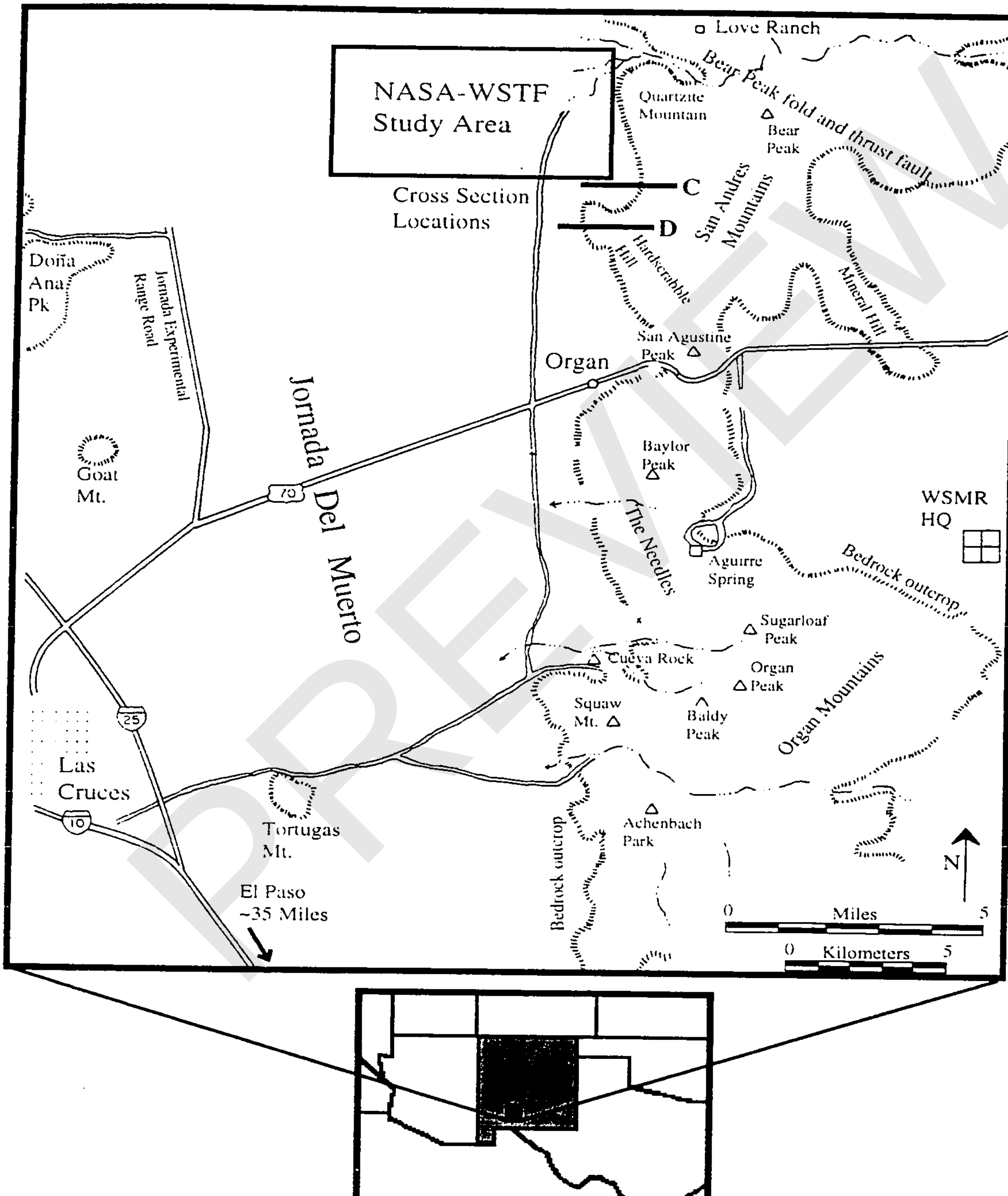

Figure 1. Index map showing the NASA White Sands Test Facility which is located 18 miles (29 km) northeast of Las Cruces, New Mexico on the western slopes of the southern San Andres Mountains (modified from Seager, 1991). The lines labeled C and D correspond to the locations of Seager's C and D cross sections.

In 1987 and 1988, approximately 42 miles (67.6 km) of shallow seismic reflection data on the NASA–WSTF were acquired for NASA by Charles B. Reynolds and Associates (CBR&A) (Reynolds and Associates, 1987, 1988) for the purpose of mapping the top of bedrock in the subsurface. The purpose of this thesis is to present the results of a re–evaluation and reinterpretation of these data in conjunction with additional geophysical and drilling data that have accumulated since acquisition of the seismic data in 1988.

The re–evaluation of the seismic data was initiated for two reasons. First, the drilling of around 100 additional monitoring wells since 1988 has led to significant discrepancies between the 1988 elevation to bedrock maps based on seismic data and elevation to bedrock as determined by the more recent monitoring wells. Differences are greatest in off–site areas where discrepancies of over 300 ft (94.1 m) can be seen in the southernmost part of the base. Second, more recent analysis of well data from within the bedrock has led to the suggestion that there may be lithologic units in the bedrock which may have important influences on regional and site–specific hydrologic processes. Of particular interest is the "Charlene shale", a Paleozoic horizon found in the eastern portion of the base that may prevent vertical migration of fluids. Subsurface mapping of this layer or other lithologic markers would give significant information on geologic structure and therefore fluid movement within the bedrock beneath the site.

In this thesis, several types of data play important roles. At the forefront are seismic reflection sections and well log information (Figures 2 and 3). The seismic lines are interpreted with the aid of top of bedrock information from the well logs. Since there are over 140 wells on the base with 88 of those penetrating into bedrock, an accurate top of bedrock map is insured. Seismic data, top of bedrock map, and well information are used to

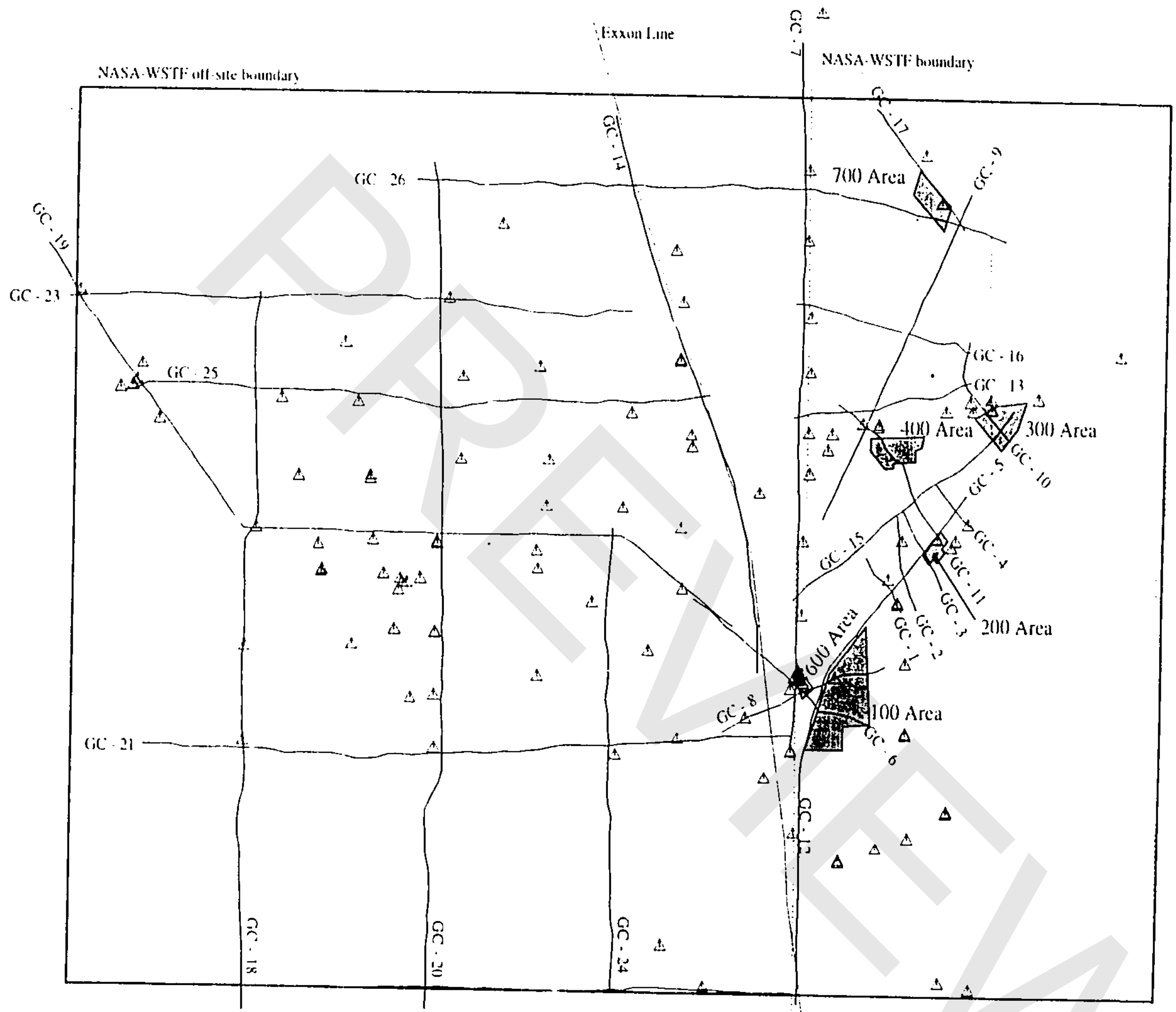

Figure 2. NASA-WSTF with location of Geoscience Consultants seismic lines (GC-1 through GC-26), contamination source areas (Area 100, 200, 300, 400, 600, and 700), and monitoring wells (⚠). The Exxon line location was obtained from Keller et al. (1986).

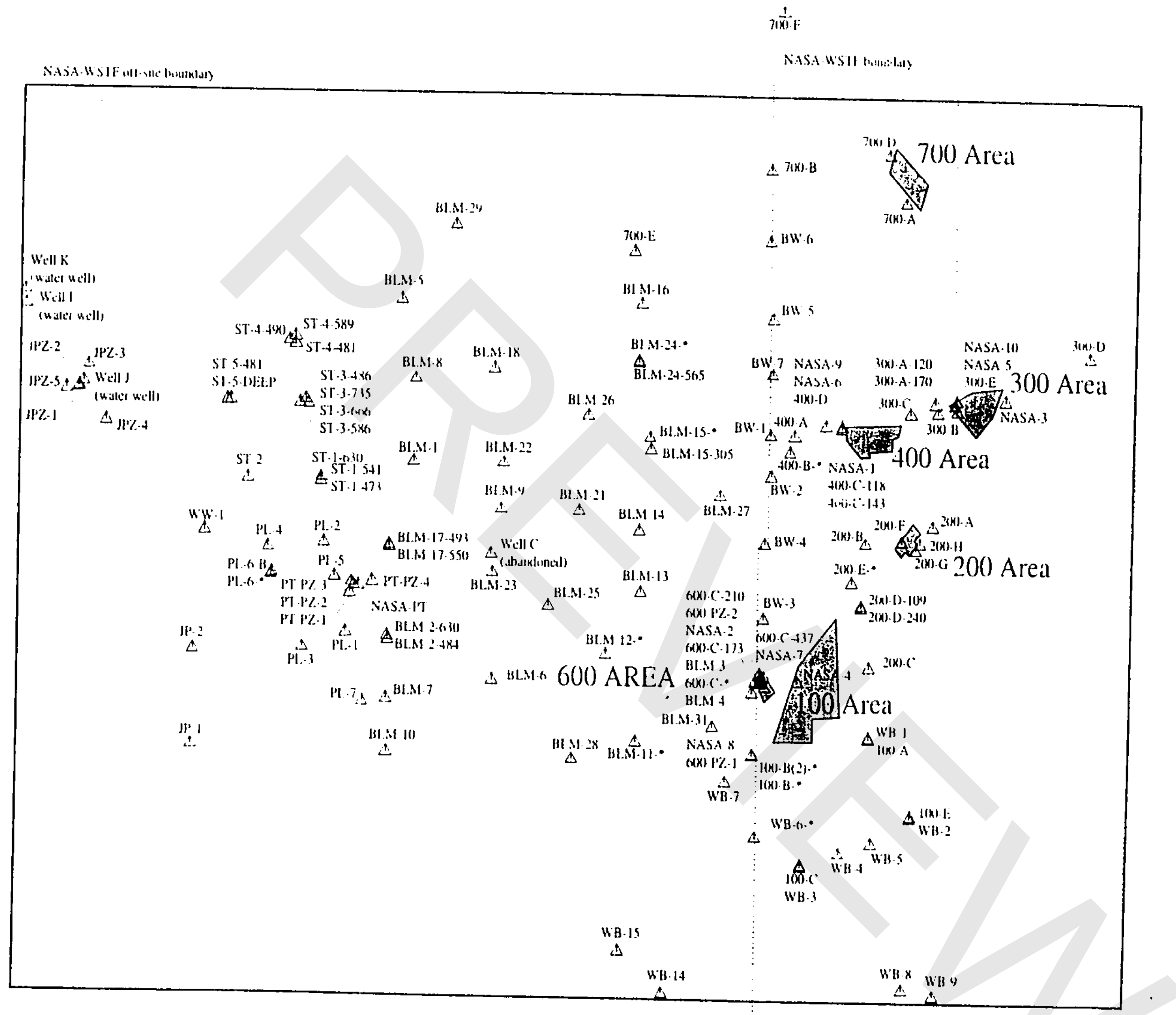

Figure 3. Water well and monitoring well locations throughout the NASA White Sands Test Facility region. There are over 140 wells, 88 of which penetrate some type of bedrock.

interpret the locations of faults, paleochannels, and any other structures which may inhibit or direct groundwater flow.

Synthetic seismograms were generated from well logs from three wells on the facility. This effort had two main goals. The first is to ensure an accurate tie between the seismic reflection sections and the top of bedrock in the wells. Sonic and density logs from these wells will be used to generate a reflection coefficient series, which in turn will generate the synthetic reflection sections. The second goal is to explore the possibility of intra–bedrock mapping on a shale layer within the Paleozoic portion of the bedrock.

New data collected as part of this thesis includes site–wide gravity and magnetic surveys, and a Vertical Seismic Profile (VSP) survey in the 600–D well. The purpose of the VSP was to provide a means of checking the velocities used in time–to–depth conversion of the seismic data. Collection of almost 85 new magnetic stations within the confines of the facility aid in the placement of very large faults and in the rough determination of the alluvial isopact and bedrock type. The addition of almost 100 new gravity stations are used in the determination of horizontal placement and vertical displacement of faults within the NASA–WSTF. Thematic Mapper images comprise the final portion of the thesis. A possibility exists that some of the buried faults may produce surface displacement. Through side looking radar imaging of the region, these faults might be detected.

In this thesis, I will present the following: 1) an updated and improved bedrock elevation map, 2) an alluvial isopach map, 3) synthetic seismograms based on well log data from from three wells in the site, 4) results of a VSP study in well 600–D, and 5) produce a complete Bouguer gravity map and magnetic intensity map based on surveys conducted during the re–evaluating period.

REGIONAL GEOLOGY

Geologic History

During latest Precambrian time, rifting and continental drift gave birth to the proto–continent of North America around 650 – 500 Ma. The rifted continental margins of interest are the Cordilleran in the west and Ouachita in the east. Throughout Early Paleozoic time both of the new continental edges accumulated thick shelf sediment. Continued passive subsidence along these margins may have allowed the margins to become connected around the southern end of a stable cratonic arch (Dickinson 1981). The southern portion of New Mexico was at the very southern tip of the this arch (Figure 4). Due to this stability of the arch and the passive tectonism during this time, the craton was eroded leaving a wide areal expanse having very little relief (Seager, 1981). Localized deposition history of central New Mexico can be seen in the stratigraphy (Figures 5 and 6).

In Late Cambrian to Early Devonian time, seas transgressed ENE across the southern tip of the arch depositing marine sediments unconformably upon the eroded Precambrian and Cambrian rocks of southern New Mexico (Seager, 1981). In the Late Paleozoic, southern New Mexico buckled under the stress produced by the Permo–Carboniferous Ouachita orogeny. Under the present day NASA–WSTF, this tectonism produced a downwarped area. At the beginning of the Permian, continued subsidence of this basin allowed shallow marine waters teeming with life to invade the region (Seager, 1981). The creatures produced mounds which were preserved in the sand and clay of the Panther Seep formation (Kottlowski, 1994).

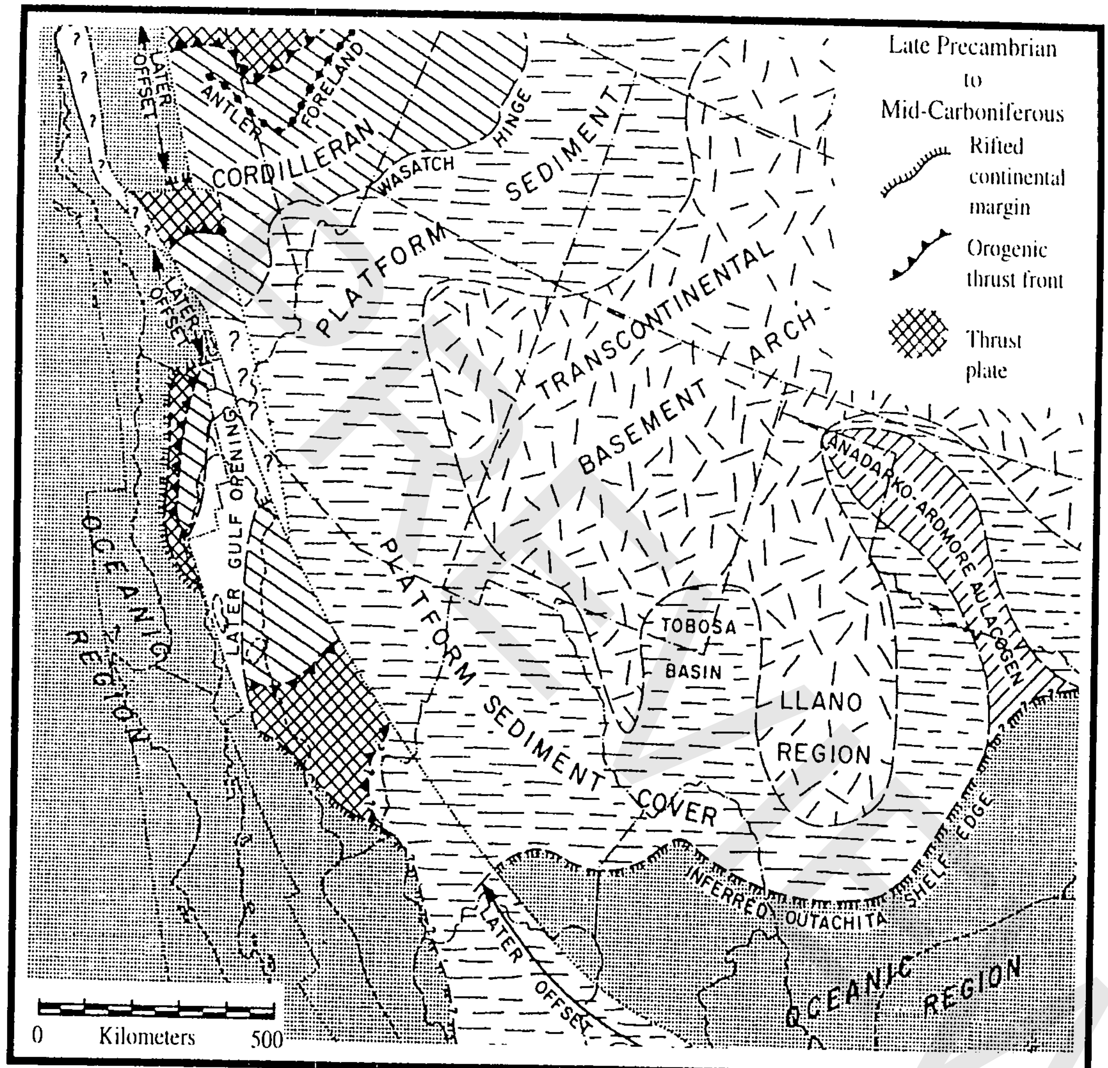

Figure 4. Paleotectonics of Southern North America during the Late Precambrian to Mid-Carboniferous. The southernmost portion of New Mexico is located on the stable basement arch, with thick platform sediment being deposited to the south. Modified from Dickinson (1981).